

Soft and virtual corrections to $pp \rightarrow H + X$ at NNLO

Robert V. Harlander* and William B. Kilgore†

*HET, Physics Department
Brookhaven National Laboratory, Upton, NY 11973, U.S.A.*

Abstract

The contributions of virtual corrections and soft gluon emission to the inclusive Higgs production cross section $pp \rightarrow H + X$ are computed at next-to-next-to-leading order in the heavy top quark limit. We show that this part of the total cross section is well behaved in the sense of perturbative convergence, with the NNLO corrections amounting to an enhancement of the NLO cross section by $\sim 5\%$ for LHC and 10-20% for the Tevatron. We compare our results with an existing estimate of the full NNLO effects and argue that an analytic evaluation of the hard scattering contributions is needed.

1 Introduction

In the last two decades the predictions of the Standard Model have been confirmed with remarkable precision. Still, the agent of electroweak symmetry breaking remains elusive. The simplest mechanism introduces a single complex scalar doublet. Three components of the doublet give mass to the W and Z bosons, leaving a single neutral particle, the Higgs boson, as the signature of the symmetry breaking sector. This scenario is called the minimal Standard Model (SM) and forms the benchmark for the investigation of electroweak symmetry breaking.

In their final run, the LEP experiments established a lower mass limit for a SM Higgs of ~ 113 GeV [1]. This value severely challenges the reach of the Tevatron. Nonetheless, there are indications that the Higgs is not much heavier than this limit. Fits to precision electroweak data actually prefer a value of the Higgs mass that is well below the exclusion limit and place a 95% confidence level upper limit near 200 GeV [2]. Supersymmetric extensions to the SM, which have at least two Higgs doublets and therefore at least five observable Higgs bosons, prefer that the mass of the lightest Higgs be below approximately 135 GeV [3]. Detailed studies indicate that, with sufficient luminosity, the Tevatron could be sensitive to Higgs bosons up to the W^+W^- threshold.

At hadron colliders, the dominant production mechanism for Higgs bosons of mass below ~ 700 GeV is gluon fusion. The Tevatron however will only be able to make limited use of this production channel. For Higgs masses well above the W^+W^- threshold, the

*email: rharlan@bnl.gov

†email: kilgore@bnl.gov

production rate is too small to be observed. For masses well below the W^+W^- threshold, the dominant $b\bar{b}$ decay mode is overwhelmed by QCD background, and the production rate is insufficient to allow observation of rare decay modes like $H \rightarrow \gamma\gamma$. Thus except for a narrow window around the W^+W^- threshold where that decay mode may be observable, the Tevatron Higgs search will rely on associated production with a W or Z boson rather than gluon fusion [4].

At the LHC the gluon fusion production mechanism will be extremely important. For lighter Higgs masses, the $b\bar{b}$ decay mode will still be overwhelmed by QCD effects, but because of the high machine luminosity and the large gluon luminosity at relatively small parton energy fractions, the LHC will be able to measure the $H \rightarrow \gamma\gamma$ decay mode. This will be important not only as a discovery channel (if the Higgs has not yet been found) but also as a means of studying Higgs properties like its coupling to top quarks.

Unfortunately, the gluon fusion process is currently not fully under control. The next-to-leading order (NLO) corrections to the production rate were computed ten years ago and were found to be extremely large, of order 70 – 100% [5, 6]. Such large corrections clearly ask for the evaluation of higher order terms in the perturbative series in order to arrive at a solid theoretical understanding of the process. In this paper, we present the soft plus virtual corrections to inclusive Higgs production at next-to-next-to-leading order (NNLO). For the relevant values of $M_H \sim 100\text{--}200$ GeV and the center-of-mass (CMS) energies at Tevatron (2 GeV) and LHC (14 TeV), these terms are not expected to dominate the full result. Nevertheless, they represent a first step towards the complete answer, in the sense that they comprise a well-defined, ultra-violet and infra-red finite, gauge and renormalization group invariant piece. By comparing to existing estimates on the NNLO corrections for $gg \rightarrow H$, we conclude that the evaluation of the full answer is necessary.

2 Higgs production through light parton scattering

2.1 Leading order

Assuming the Standard Model as the theory of particle interactions, the coupling of the Higgs boson to gluons is mediated by a quark loop. In the following we will neglect all quark masses except for the top mass. In this case only the top quark contributes, because the Yukawa couplings are proportional to the fermion masses. The lowest order diagram is then shown in Fig. 1 (a). It was computed some time ago [7] and leads to the cross section

$$\begin{aligned} \sigma_{\text{LO}}(gg \rightarrow H) &= \frac{G_F \alpha_s^2(\mu^2)}{128\sqrt{2}\pi} \tau^2 \delta(1-x) |1 + (1-\tau)f(\tau)|^2, \\ f(\tau) &= \begin{cases} \arcsin^2 \frac{1}{\sqrt{\tau}}, & \tau \geq 1, \\ -\frac{1}{4} \left[\ln \frac{1+\sqrt{1-\tau}}{1-\sqrt{1-\tau}} - i\pi \right]^2, & \tau < 1, \end{cases} \\ \tau &= 4M_t^2/M_H^2, \quad x = M_H^2/s, \end{aligned} \tag{1}$$

where s is the partonic center-of-mass energy, G_F the Fermi coupling constant, α_s the strong coupling constant (which depends on the renormalization scale μ), M_t the pole mass of the top quark, and M_H the Higgs mass.

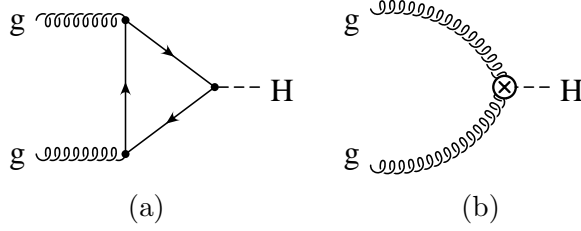


Figure 1: Leading order diagram to the process $gg \rightarrow H$: (a) in full QCD; (b) in the effective theory (Eq. (2)). The straight solid lines represent the top quark, the symbol \otimes denotes the effective vertex.

2.2 Effective Lagrangian

The lowest threshold of the diagram in Fig. 1 (a) is at $M_H = 2M_t$. This means that an expansion in terms of M_H/M_t is expected to converge for $M_H < 2M_t$. In fact, it has been shown that the NLO K-factor for this process is excellently approximated up to much larger Higgs masses, even by keeping only the first term of such an expansion. With a top mass of around $M_t = 175$ GeV and the experimental data favoring a relatively low Higgs mass between 100 to 200 GeV, we feel that keeping only the leading term in M_H/M_t is also well justified at NNLO.

We therefore integrate out the top quark and compute amplitudes using QCD with five active flavors and the following effective Lagrangian [8] for the Higgs-gluon interaction:

$$\mathcal{L}_{\text{eff}} = -\frac{H}{4v} C_1 \mathcal{O}_1 = -\frac{H}{4v} C_1^{\text{B}} \mathcal{O}_1^{\text{B}}, \quad \mathcal{O}_1 = G_{\mu\nu}^a G^{a\mu\nu}, \quad (2)$$

where $G_{\mu\nu}^a$ is the gluon field strength tensor. In the approximation that all light flavors are massless, this effective Lagrangian is renormalization group invariant, but the coefficient function C_1^{B} and the operator \mathcal{O}_1^{B} must each be renormalized. Below, we give the renormalized value of C_1 while the renormalization of \mathcal{O}_1^{B} and its matrix elements is discussed in Sect. 3.1.

The coefficient function contains the residual logarithmic dependence on the top quark mass and has been computed up to $\mathcal{O}(\alpha_s^4)$ [9]. For our purposes, we need it only up to $\mathcal{O}(\alpha_s^3)$ [9, 10]. The $\overline{\text{MS}}$ renormalized coefficient function is:

$$C_1 = -\frac{1}{3} \frac{\alpha_s}{\pi} \left\{ 1 + \frac{11}{4} \frac{\alpha_s}{\pi} + \left(\frac{\alpha_s}{\pi} \right)^2 \left[\frac{2777}{288} + \frac{19}{16} l_t + n_f \left(-\frac{67}{96} + \frac{1}{3} l_t \right) \right] + \dots \right\}, \quad (3)$$

where $l_t = \ln(\mu^2/M_t^2)$ and M_t the on-shell top quark mass. $\alpha_s \equiv \alpha_s^{(5)}(\mu^2)$ is the $\overline{\text{MS}}$ renormalized QCD coupling constant for five active flavors, and n_f is the number of massless flavors. In our numerical results, we always set $n_f = 5$.

Using the effective Lagrangian of Eq. (2), the lowest order amplitude for the process $gg \rightarrow H$ reduces from the one-loop diagram in Fig. 1 (a) to the tree-level diagram in Fig. 1 (b).

2.3 Sub-Processes: virtual, single real, double real

For a complete treatment of the process $pp \rightarrow H$ in NNLO QCD one needs to compute the partonic processes which must then be convoluted with parton distribution functions.

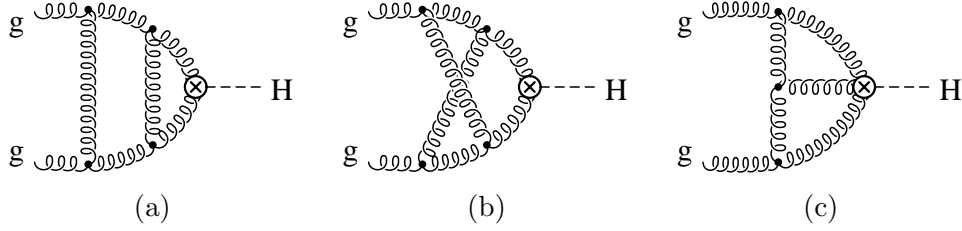


Figure 2: Sample two-loop diagrams contributing to the virtual corrections at NNLO.

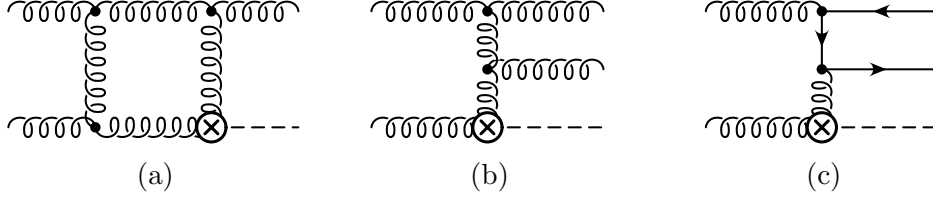


Figure 3: Typical diagrams contributing to (a) single and (b) double real radiation of gluons and (c) double real radiation of quark-antiquark pairs at NNLO. The dashed line is the Higgs boson and “ \otimes ” denotes the effective Higgs-gluon vertex.

The partonic subprocesses are:

- (i) Virtual corrections to two loops:
 $gg \rightarrow H$
- (ii) Single real radiation to one loop:
 $gg \rightarrow Hg$, $q\bar{q} \rightarrow Hg$, $qg \rightarrow Hq$, $\bar{q}g \rightarrow H\bar{q}$
- (iii) Double real radiation at tree level:
 $gg \rightarrow Hgg$, $gg \rightarrow Hq\bar{q}$, $q\bar{q} \rightarrow Hgg$, $q\bar{q} \rightarrow Hq\bar{q}$, $qg \rightarrow Hqg$, $\bar{q}g \rightarrow H\bar{q}g$

2.4 The Soft Approximation

Radiative corrections to inclusive production fall into three categories: delta function terms $\propto \delta(1-x)$, large logarithms of the form $\ln^n(1-x)/(1-x)$, and hard scattering terms that have at most a logarithmic singularity as $x \rightarrow 1$, where x is the ratio of the Higgs boson mass squared to the incoming parton CMS energy squared (see Eq. (1)). In the kinematically similar Drell-Yan process [11] and in inclusive Higgs production at NLO [5], it has been observed that the delta function and large log terms are important though not necessarily dominant parts of the radiative corrections.

Virtual corrections add only delta function contributions while real emission corrections contribute to all three categories. The soft approximation is obtained by taking the limit $x \rightarrow 1$. In doing so, one is left with only those terms that scale like $(1-x)^{-1-a\epsilon}$, where $\epsilon = (4-d)/2$, and d is the number of space-time dimensions assumed for the regularization of divergent integrals. The term $(1-x)^{-1-a\epsilon}$ must be interpreted as a distribution,

$$f_{a\epsilon}(x) \equiv -a\epsilon (1-x)^{-1-a\epsilon} = \delta(1-x) + \sum_{n=0}^{\infty} \frac{(-a\epsilon)^{n+1}}{n!} \mathcal{D}_n(x), \quad (4)$$

where $\mathcal{D}_n(x)$ is a “plus” distribution,

$$\mathcal{D}_n(x) = \left[\frac{\ln^n(1-x)}{1-x} \right]_+, \quad (5)$$

$$\int_0^1 dx h(x) \mathcal{D}_n(x) = \int_0^1 dx [h(x) - h(1)] \frac{\ln^n(1-x)}{1-x}.$$

Thus, towers of the large logarithm terms $\mathcal{D}_n(x)$ can be trivially obtained from knowledge of the $\delta(1-x)$ terms.

3 Results

3.1 Renormalization of matrix elements

We write the partonic cross section as follows:

$$\sigma = \frac{\pi}{64v^2} C_1^2(\alpha_s) Z_1^2(\alpha_s) \frac{1}{(1-\epsilon)^2} [\rho_A + \rho_B + \rho_C]. \quad (6)$$

ρ_A is the contribution from virtual corrections, while ρ_B and ρ_C represent the contributions from single and double real emission, respectively. $Z_1(\alpha_s)$ is the global renormalization factor for the composite operator in the effective Lagrangian [12]:

$$\mathcal{O}_1 = Z_1(\alpha_s) \mathcal{O}_1^B, \quad (7)$$

with $Z_1(\alpha_s) = \frac{1}{1 - \beta(\alpha_s)/\epsilon} = 1 - \frac{\alpha_s}{\pi} \frac{\beta_0}{\epsilon} + \left(\frac{\alpha_s}{\pi} \right)^2 \left[\frac{\beta_0^2}{\epsilon^2} - \frac{\beta_1}{\epsilon} \right] + \mathcal{O}(\alpha_s^3).$

Here, $\beta(\alpha_s)$ is the QCD beta function:

$$\beta(\alpha_s) = -\frac{\alpha_s}{\pi} \beta_0 - \left(\frac{\alpha_s}{\pi} \right)^2 \beta_1 + \mathcal{O}(\alpha_s^3), \quad (8)$$

$$\beta_0 = \frac{1}{4} \left(11 - \frac{2}{3} n_f \right), \quad \beta_1 = \frac{1}{16} \left(102 - \frac{38}{3} n_f \right).$$

In the following sections, we will list the results for ρ_A , ρ_B , and ρ_C in terms of the bare coupling α_s^B which is related to the $\overline{\text{MS}}$ renormalized coupling by

$$\alpha_s^B = \mathcal{N}^{-1} Z_\alpha(\alpha_s) \alpha_s, \quad (9)$$

where $\mathcal{N} \equiv \exp[\epsilon(-\gamma_E + \ln 4\pi)],$

and $\gamma_E = 0.577216\dots$ is the Euler constant. The charge renormalization constant $Z_\alpha(\alpha_s)$ is

$$Z_\alpha(\alpha_s) = 1 - \frac{\alpha_s}{\pi} \frac{\beta_0}{\epsilon} + \left(\frac{\alpha_s}{\pi} \right)^2 \left(\frac{\beta_0^2}{\epsilon^2} - \frac{\beta_1}{2\epsilon} \right) + \mathcal{O}(\alpha_s^3). \quad (10)$$

3.2 Two-loop virtual corrections

The two-loop virtual corrections have been calculated in [13]. Typical diagrams are shown in Fig. 2. Since gluons are massless, these diagrams depend on only a single scale $q^2 = M_H^2$, where q is the momentum of the Higgs boson. They were calculated using the method of ref. [14] which allows one to relate the integration-by-parts identities for the two-loop three-point functions of Fig. 2 to those for three-loop two-point functions [15]. The coding of the integration routines was done in FORM [16] and was based on the program MINCER [17]. It is worth mentioning that the resulting program is capable of dealing with much more general diagrams than the ones considered for this calculation. In particular it solves integrals with (in principle) arbitrary integer powers of the propagators. This may become useful in future applications where expansions have to be applied to the diagrams.

The expression for ρ_A is given in ref. [13]:

$$\rho_A = \rho_A^{(0)} + \frac{\alpha_s^B}{\pi} \rho_A^{(1)} + \left(\frac{\alpha_s^B}{\pi} \right)^2 \rho_A^{(2)} + \mathcal{O}(\alpha_s^3), \quad (11)$$

$$\begin{aligned} \rho_A^{(0)}(x) &= (1 - \epsilon) \delta(1 - x), \\ \rho_A^{(1)}(x) &= \mathcal{N} \left(\frac{\mu^2}{M_H^2} \right)^\epsilon \delta(1 - x) \left[-\frac{3}{\epsilon^2} + \frac{3}{\epsilon} + \frac{21}{2} \zeta_2 + \epsilon \left(-3 - \frac{21}{2} \zeta_2 + 7 \zeta_3 \right) \right], \\ \rho_A^{(2)}(x) &= \mathcal{N}^2 \left(\frac{\mu^2}{M_H^2} \right)^{2\epsilon} \delta(1 - x) \left\{ \frac{9}{2\epsilon^4} + \frac{1}{\epsilon^3} \left(-\frac{105}{16} + \frac{1}{8} n_f \right) \right. \\ &\quad + \frac{1}{\epsilon^2} \left(-\frac{17}{8} - \frac{243}{8} \zeta_2 + \frac{1}{12} n_f \right) \\ &\quad + \frac{1}{\epsilon} \left[\frac{553}{48} + \frac{981}{16} \zeta_2 - \frac{159}{8} \zeta_3 + n_f \left(-\frac{53}{72} - \frac{15}{8} \zeta_2 \right) \right] \\ &\quad \left. + \frac{6749}{144} + \frac{255}{8} \zeta_2 + \frac{85}{4} \zeta_3 + \frac{1161}{20} \zeta_2^2 + n_f \left(-\frac{137}{27} - \frac{5}{4} \zeta_2 - \frac{7}{4} \zeta_3 \right) \right\}, \end{aligned} \quad (12)$$

where $\zeta_n \equiv \zeta(n)$ is Riemann's ζ function which takes the particular values

$$\begin{aligned} \zeta_2 &= \pi^2/6 = 1.64493\dots \\ \zeta_3 &= 1.20206\dots \end{aligned} \quad (13)$$

3.3 Single real radiation

The one-loop amplitudes for the processes (ii) in Sect. 2.3 were computed in ref. [18] in the form of helicity amplitudes to order ϵ^0 . Unfortunately, these amplitudes are not sufficient for our purpose. The integration over two-particle phase space generates infrared singularities which take the form of single and double poles in ϵ which combine with the $\mathcal{O}(\epsilon)$ and $\mathcal{O}(\epsilon^2)$ pieces of the amplitude to produce finite contributions to the cross section. If we were to work in the Four Dimensional Helicity scheme [19], where gluons have two polarization states, helicity amplitudes extended to higher order in ϵ would suffice. However, since we work in the Conventional Dimensional Regularization scheme, gluons have $d - 2 = 2 - 2\epsilon$ polarizations. Thus, in addition to helicity amplitudes we also need

amplitudes corresponding to the extra “ ϵ ” polarizations. Both the extra pieces of the amplitudes and the integration over the two-particle phase space have been performed in reference [20]. This calculation includes the full dependence on the center-of-mass energy. Here we are interested in the soft limit, to which we find that only the $gg \rightarrow Hg$ process contributes. The result is:

$$\rho_B = \frac{\alpha_s^B}{\pi} \rho_B^{(1)} + \left(\frac{\alpha_s^B}{\pi} \right)^2 \rho_B^{(2)} + \mathcal{O}(\alpha_s^3), \quad (14)$$

$$\begin{aligned} \rho_B^{(1)}(x) &= \mathcal{N} \left(\frac{\mu^2}{M_H^2} \right)^\epsilon f_{2\epsilon}(x) \left[\frac{3}{\epsilon^2} - \frac{3}{\epsilon} - \frac{9}{2} \zeta_2 + \epsilon \left(\frac{9}{2} \zeta_2 - 7 \zeta_3 \right) \right], \\ \rho_B^{(2)}(x) &= \mathcal{N}^2 \left(\frac{\mu^2}{M_H^2} \right)^{2\epsilon} \left\{ f_{2\epsilon}(x) \left[-\frac{9}{\epsilon^4} + \frac{9}{\epsilon^3} + \frac{45}{\epsilon^2} \zeta_2 \right. \right. \\ &\quad \left. \left. + \frac{1}{\epsilon} (-9 - 45 \zeta_2 + 42 \zeta_3) - 18 - 42 \zeta_3 - \frac{603}{10} \zeta_2^2 \right] \right. \\ &\quad \left. + f_{4\epsilon}(x) \left[-\frac{9}{8\epsilon^4} + \frac{9}{8\epsilon^3} + \frac{63}{8\epsilon^2} \zeta_2 + \frac{1}{\epsilon} \left(-\frac{63}{8} \zeta_2 + 21 \zeta_3 \right) - 21 \zeta_3 + \frac{189}{80} \zeta_2^2 \right] \right\}. \end{aligned} \quad (15)$$

Expanding $f_{a\epsilon}(x)$ (see Eq. (4)), Eq. (15) describes both delta function and large logarithm contributions to the radiative corrections.

3.4 Double real radiation

The tree-level amplitudes for the processes (*iii*) of Sect. 2.3 with two partons in the final state was evaluated in [21], though again only as helicity amplitudes to $\mathcal{O}(\epsilon^0)$. We have evaluated the full ϵ dependence in the conventional dimensional regularization scheme by computing all of the Feynman diagrams, squaring the amplitude and integrating over phase space, dropping terms that do not contribute in the soft limit as described in Sect. 2.4. We find that only the $gg \rightarrow Hgg$ and $gg \rightarrow Hq\bar{q}$ processes contribute with the result

$$\begin{aligned} \rho_C(x) &= \mathcal{N}^2 \left(\frac{\alpha_s^B}{\pi} \right)^2 \left(\frac{\mu^2}{M_H^2} \right)^{2\epsilon} f_{4\epsilon}(x) \left\{ \frac{45}{8\epsilon^4} - \frac{57}{16\epsilon^3} + \frac{1}{\epsilon^2} \left(\frac{17}{8} - \frac{81}{2} \zeta_2 \right) \right. \\ &\quad \left. + \frac{1}{\epsilon} \left(\frac{203}{48} + \frac{417}{16} \zeta_2 - \frac{975}{8} \zeta_3 \right) + \frac{76}{9} - \frac{119}{8} \zeta_2 + \frac{317}{4} \zeta_3 - \frac{333}{80} \zeta_2^2 \right. \\ &\quad \left. + n_f \left[-\frac{1}{8\epsilon^3} - \frac{1}{12\epsilon^2} + \frac{1}{\epsilon} \left(-\frac{13}{72} + \frac{7}{8} \zeta_2 \right) - \frac{10}{27} + \frac{7}{12} \zeta_2 + \frac{31}{12} \zeta_3 \right] \right\} + \mathcal{O}(\alpha_s^3). \end{aligned} \quad (16)$$

The terms proportional to n_f come from the $gg \rightarrow Hq\bar{q}$ sub-process.

3.5 Mass factorization

After combining all processes and renormalizing, there are still infrared singularities left over. These are all associated with mass factorization and can be absorbed into process independent functions $\Gamma_{ij}(x)$ associated with the incoming partons. The (IR-finite) partonic

cross section, $\hat{\sigma}$, is defined implicitly by the relation

$$\sigma_{ij} = \sum_{\bar{i}, \bar{j}} \hat{\sigma}_{\bar{i}\bar{j}} \otimes \Gamma_{\bar{i}} \otimes \Gamma_{\bar{j}j}, \quad (17)$$

where σ is defined in Eq. (6). The symbol \otimes indicates convolution over longitudinal momentum fractions,

$$(f \otimes g)(x) = \int_0^1 dy \int_0^1 dz f(y) g(z) \delta(x - yz), \quad (18)$$

and the subscripts \bar{i} , i , etc., indicate parton identities. The $\Gamma_{ij}(x)$'s are given by

$$\begin{aligned} \Gamma_{ij}(x) = & \delta_{ij} \delta(1-x) - \frac{\alpha_s}{\pi} \frac{P_{ij}^{(0)}(x)}{\epsilon} \\ & + \left(\frac{\alpha_s}{\pi}\right)^2 \left[\frac{1}{2\epsilon^2} \left((P_{ik}^{(0)} \otimes P_{kj}^{(0)})(x) + \beta_0 P_{ij}^{(0)}(x) \right) - \frac{1}{2\epsilon} P_{ij}^{(1)}(x) \right] + \mathcal{O}(\alpha_s^3), \end{aligned} \quad (19)$$

where the $P_{ij}^{(n)}$ are the n th order splitting functions [22, 23]. In the soft limit, only $P_{ij}^{(n)}$ with $i = j = g$ contribute. They are given by

$$\begin{aligned} P_{gg}^{(0)}(x) & \xrightarrow{\text{soft}} \left(\frac{11}{4} - \frac{n_f}{6} \right) \delta(1-x) + 3 \mathcal{D}_0(x), \\ P_{gg}^{(1)}(x) & \xrightarrow{\text{soft}} \left(6 + \frac{27}{4} \zeta_3 - \frac{2}{3} n_f \right) \delta(1-x) + \left(\frac{67}{4} - \frac{9}{2} \zeta_2 - \frac{5}{6} n_f \right) \mathcal{D}_0(x). \end{aligned} \quad (20)$$

Writing

$$\sigma_{gg} = \sigma_{gg}^{(0)} + \frac{\alpha_s}{\pi} \sigma_{gg}^{(1)} + \left(\frac{\alpha_s}{\pi}\right)^2 \sigma_{gg}^{(2)} + \dots, \quad (21)$$

and similarly for $\hat{\sigma}_{gg}$, Eq. (17) can be solved for $\hat{\sigma}_{gg}$ order by order to give

$$\begin{aligned} \hat{\sigma}_{gg}^{(0)}(x) & = \sigma_{gg}^{(0)}(x) \equiv \sigma_0 \delta(1-x), \\ \hat{\sigma}_{gg}^{(1)}(x) & = \sigma_{gg}^{(1)}(x) + 2\sigma_0 P_{gg}^{(0)}(x) \frac{1}{\epsilon}, \\ \hat{\sigma}_{gg}^{(2)}(x) & = \sigma_{gg}^{(2)}(x) - \frac{1}{\epsilon^2} \sigma_0 \left(\beta_0 P_{gg}^{(0)}(x) + 2(P_{gg}^{(0)} \otimes P_{gg}^{(0)})(x) \right) \\ & \quad + \frac{1}{\epsilon} \left(\sigma_0 P_{gg}^{(1)}(x) + 2(P_{gg}^{(0)} \otimes \hat{\sigma}_{gg}^{(1)})(x) \right), \end{aligned} \quad (22)$$

where

$$\sigma_0 \equiv \frac{\pi}{576v^2} \left(\frac{\alpha_s}{\pi} \right)^2 (1 + \epsilon + \epsilon^2). \quad (23)$$

The convolutions in Eq. (22) can be evaluated with the help of the following relations

$$\begin{aligned} (\mathcal{D}_0 \otimes \mathcal{D}_0)(x) & \xrightarrow{\text{soft}} -\zeta_2 \delta(1-x) + 2\mathcal{D}_1(x), \\ (\mathcal{D}_0 \otimes \mathcal{D}_1)(x) & \xrightarrow{\text{soft}} \zeta_3 \delta(1-x) - \zeta_2 \mathcal{D}_0(x) + \frac{3}{2} \mathcal{D}_2(x), \\ (\mathcal{D}_0 \otimes \mathcal{D}_2)(x) & \xrightarrow{\text{soft}} -\frac{4}{5} \zeta_2^2 \delta(1-x) + 2\zeta_3 \mathcal{D}_0(x) - 2\zeta_2 \mathcal{D}_1(x) + \frac{4}{3} \mathcal{D}_3(x), \\ (\mathcal{D}_1 \otimes \mathcal{D}_1)(x) & \xrightarrow{\text{soft}} -\frac{1}{10} \zeta_2^2 \delta(1-x) - 2\zeta_2 \mathcal{D}_1(x) + \mathcal{D}_3(x). \end{aligned} \quad (24)$$

3.6 Partonic cross section

Putting things together, we finally arrive at

$$\begin{aligned}
\hat{\sigma}_{gg}^{(0)} &= \frac{\pi}{576v^2} \left(\frac{\alpha_s}{\pi} \right)^2 \delta(1-x), \\
\hat{\sigma}_{gg}^{(1),\text{soft}} &= \frac{\pi}{576v^2} \left(\frac{\alpha_s}{\pi} \right)^3 \left\{ \delta(1-x) \left[\frac{11}{2} + 6\zeta_2 \right] - 6\mathcal{D}_0(x)l_H + 12\mathcal{D}_1(x) \right\}, \\
\hat{\sigma}_{gg}^{(2),\text{soft}} &= \frac{\pi}{576v^2} \left(\frac{\alpha_s}{\pi} \right)^4 \left\{ \delta(1-x) \left[\frac{11399}{144} + \frac{133}{2}\zeta_2 - \frac{165}{4}\zeta_3 - \frac{9}{20}\zeta_2^2 \right. \right. \\
&\quad \left. \left. + \left(\frac{27}{2} + \frac{33}{2}\zeta_2 - \frac{171}{2}\zeta_3 \right) l_H - 18\zeta_2 l_H^2 + \frac{19}{8}l_t \right. \right. \\
&\quad \left. \left. + n_f \left(-\frac{1189}{144} - \frac{5}{3}\zeta_2 + \frac{5}{6}\zeta_3 + \left(-\frac{11}{6} - \zeta_2 \right) l_H + \frac{2}{3}l_t \right) \right] \right. \\
&\quad \left. + \mathcal{D}_0(x) \left[-\frac{101}{3} + 33\zeta_2 + \frac{351}{2}\zeta_3 + \left(-\frac{133}{2} + 45\zeta_2 \right) l_H - \frac{33}{4}l_H^2 \right. \right. \\
&\quad \left. \left. + n_f \left(\frac{14}{9} - 2\zeta_2 + \frac{5}{3}l_H + \frac{1}{2}l_H^2 \right) \right] \right. \\
&\quad \left. + \mathcal{D}_1(x) \left[133 - 90\zeta_2 + 33l_H + 36l_H^2 + n_f \left(-\frac{10}{3} - 2l_H \right) \right] \right. \\
&\quad \left. + \mathcal{D}_2(x) [-33 - 108l_H + 2n_f] + 72\mathcal{D}_3(x) \right\}, \tag{25}
\end{aligned}$$

with $l_H \equiv \ln(\mu^2/M_H^2)$ and $l_t \equiv \ln(\mu^2/M_t)$. As a numerical example, let us set $\mu^2 = M_H^2$ and insert the values $M_H = 130 \text{ GeV}$, $M_t = 175 \text{ GeV}$, and $\alpha_s = 0.112$:

$$\begin{aligned}
\hat{\sigma}_{gg} &= \frac{\pi}{576v^2} \left(\frac{\alpha_s}{\pi} \right)^2 \left\{ [1 + 0.548 + 0.107] \delta(1-x) + [0 + 0 + 0.283] \mathcal{D}_0(x) \right. \\
&\quad \left. + [0 + 0.428 - 0.040] \mathcal{D}_1(x) + [0 + 0 - 0.029] \mathcal{D}_2(x) \right. \\
&\quad \left. + [0 + 0 + 0.092] \mathcal{D}_3(x) \right\} + \mathcal{O}(\alpha_s^5), \tag{26}
\end{aligned}$$

where the individual numbers in square brackets correspond to the $\hat{\sigma}_{gg}^{(0)}$, $\hat{\sigma}_{gg}^{(1)}$, and $\hat{\sigma}_{gg}^{(2)}$ contributions. We observe that the coefficient of the δ function exhibits satisfactory convergence behavior. The magnitude of its NNLO contribution agrees roughly with the estimate of ref. [13].

3.6.1 Checks on the Result

There are several checks that can be performed on our result. The first check is to observe that all poles in ϵ cancel to give us a finite result for $\hat{\sigma}_{gg}^{(2),\text{soft}}$. Since the $\mathcal{D}_n(x)$ terms at order ϵ^0 are linked to the poles of the real emission contributions, this already gives us great confidence in these terms. Below we will discuss an even more stringent constraint on the \mathcal{D}_n coefficients.

Another check is to compare the three leading poles of the virtual two-loop corrections to the general result of ref. [24], where they are expressed in terms of universal functions

that depend only on the identity of the external partons. The poles of the diagrammatic result of [13] fully obey this observation [25].

One can now combine the universal (three leading) NNLO pole terms with the NLO results $\rho_A^{(0,1)}$ and $\rho_B^{(1)}$ to derive the coefficients of $\mathcal{D}_n(x)$ for $n = 1, 2, 3$ in $\hat{\sigma}_{gg}^{(2),\text{soft}}$. Note that this uses only one-loop results and the universal behavior of QCD amplitudes and is done without reference to any of the newly calculated NNLO terms (including those of [13]). The pole structure of the real radiation terms must take the form

$$\begin{aligned} \left(\rho_B^{(2)} + \rho_C^{(2)}\right)_{\text{pole}} &= f_{2\epsilon}(x) \left(\frac{\mu^2}{M_H^2}\right)^{2\epsilon} \left[\frac{a_{24}}{\epsilon^4} + \frac{a_{23}}{\epsilon^3} + \frac{a_{22}}{\epsilon^2} + \frac{a_{21}}{\epsilon} \right] \\ &+ f_{4\epsilon}(x) \left(\frac{\mu^2}{M_H^2}\right)^{2\epsilon} \left[\frac{a_{44}}{\epsilon^4} + \frac{a_{43}}{\epsilon^3} + \frac{a_{42}}{\epsilon^2} + \frac{a_{41}}{\epsilon} \right]. \end{aligned} \quad (27)$$

Expanding the $f_{n\epsilon}(x)$ terms as in Eq. (4) and requiring that all poles vanish from $\hat{\sigma}_{gg}^{(2)}$, we can solve for a_{n4} , a_{n3} and a_{n2} ($n = 2, 4$), while a_{21} and a_{41} remain undetermined. This solution is sufficient to fix the coefficients of $\mathcal{D}_1(x)$, $\mathcal{D}_2(x)$ and $\mathcal{D}_3(x)$ in $\hat{\sigma}_{gg}^{(2)}$, though not the coefficient of $\mathcal{D}_0(x)$. We find complete agreement between the $\mathcal{D}_{\{3,2,1\}}$ terms determined in this way and those found in Eq. (25).

Let us note that the absence of terms $\propto f_{n\epsilon}$ with $n \neq 2, 4$ in Eq. (27) can be understood from the following consideration. The index n of the $f_{n\epsilon}$ terms has two sources: the phase space elements for single and double real radiation contribute factors of $(1-x)^{1-2\epsilon}$ and $(1-x)^{3-4\epsilon}$ respectively (see *e.g.* Appendix E of ref. [11]), while the one-loop corrections to single real radiation amplitudes squared can contribute factors of $(1-x)^m$, $(1-x)^{m-\epsilon}$ or $(1-x)^{m-2\epsilon}$, where m is an integer [18, 20]. (Tree-level amplitudes squared contain only integer powers of $(1-x)$.) The $(1-x)^{-2-\epsilon}$ terms in the one-loop amplitude squared should generate an $f_{3\epsilon}(x)$ contribution. However, the universal functions describing the soft factorization properties of one-loop amplitudes only contain terms that scale like $(1-x)^{-1}$ and $(1-x)^{-1-2\epsilon}$ [26]. Thus, there are no terms in the squared amplitude that scale like $(1-x)^{-2-\epsilon}$ and that survive the soft limit.

Another way to derive the $\mathcal{D}_{\{1,2,3\}}(x)$ terms without using any process-specific NNLO results is to perform a threshold resummation analysis along the lines of [27]. Again we find complete agreement with our result. As a by-product, we can use our result for the coefficient of \mathcal{D}_0 in order to derive additional input for the resummation formula. Of particular interest is the NNLO coefficient attributed to large-angle soft-gluon emissions which has been derived for the Drell-Yan and deep inelastic scattering processes in ref. [28] (where it is called D_2^P , $P = \text{DY, DIS, } \dots$). Following this analysis for $gg \rightarrow H$, one finds that the corresponding coefficient can be obtained from the one in the Drell-Yan process (Eq. (21) in [28]) simply by changing the color factor C_F to C_A .¹ This suggests that the coefficient D_2^P of [28] is universal in nature.

A further check concerns the terms proportional to $\ln \mu^2$ which can be derived from renormalization group and factorization scale invariance of the physical cross section:²

$$\sigma_{pp} = \hat{\sigma}_{gg} \otimes g \otimes g, \quad (28)$$

¹We thank W. Vogelsang for pointing this out to us.

²Note that we restrict ourselves to the limit of soft gluons.

where g is the gluon distribution function. This leads to

$$\mu^2 \frac{d}{d\mu^2} \hat{\sigma}_{gg} + 2 \left[\frac{\alpha_s}{\pi} P_{gg}^{(0)} + \left(\frac{\alpha_s}{\pi} \right)^2 P_{gg}^{(1)} \right] \otimes \hat{\sigma}_{gg} = \mathcal{O}(\alpha_s^5). \quad (29)$$

Eq. (25) satisfies this relation.

4 Discussion

For a consistent discussion of the physical implications at NNLO, one has to convolute the partonic cross section at a given order with the corresponding parton distribution functions (PDFs) of the same order. Unfortunately, NNLO PDFs are not yet available.³ Thus, we will restrict ourselves to a semi-quantitative investigation of the NNLO effects by using NLO PDFs at NNLO. In all results we have used the CTEQ5 [29] family of parton distributions.

We define

$$K_{\text{NLO}} = \frac{\sigma_{\text{NLO}}}{\sigma_{\text{LO}}}, \quad K_{\text{NNLO}} = \frac{\tilde{\sigma}_{\text{NNLO}}}{\sigma_{\text{LO}}}, \quad (30)$$

where $\tilde{\sigma}_{\text{NNLO}}$ is obtained by convoluting the partonic $\hat{\sigma}_{gg}^{(2)}$ with NLO PDFs and using NLO evolution of the strong coupling constant. σ_{LO} and σ_{NLO} are evaluated consistently with LO and NLO PDFs and α_s evolution, respectively. Of course the treatment for K_{NNLO} is inconsistent, but one may nevertheless get an idea on the magnitude of the effects.

Fig. 4 shows the K -factors K_{NLO} and K_{NNLO} for a proton-proton CMS energy of (a) 14 TeV and (b) 2 TeV, when only the purely soft terms (*i.e.* $\propto \delta(1-x)$ and $\propto \mathcal{D}_n(x)$) are kept. One finds a nicely convergent behavior when going from NLO to NNLO, both for LHC and Tevatron energies. Also shown are the approximate soft NNLO terms of [10] (see below).

Fig. 5 shows the cross section $\sigma(pp \rightarrow H + X)$ obtained by weighting the terms in Eq. (25) by the ratio of the LO expression for $\hat{\sigma}$ in the heavy top limit with the LO result including full top mass dependence given in Eq.(1). This procedure has been shown to be an excellent approximation of the full top mass dependence at NLO for Higgs masses up to and even beyond the top threshold. These curves again demonstrate the nice convergence of the soft contributions to the cross section.

Note that these numbers do not represent the full phenomenological result, because of the missing, non-negligible contributions coming from hard scattering. Rather, this consistent comparison of the soft limits at NLO and NNLO should give an indication of the magnitude of the total corrections.

4.1 Estimating the hard scattering contributions

At NLO one finds that the soft corrections, while significant, are by no means dominant. Comparison of the dashed lines in Fig. 4 to those of Fig. 6 (discussed below), shows that the soft terms account for no more than half (and often significantly less) of the total NLO

³Various necessary ingredients are already available, and it seems to be clear that the combined efforts of different groups will eventually result in an appropriate set of distributions.

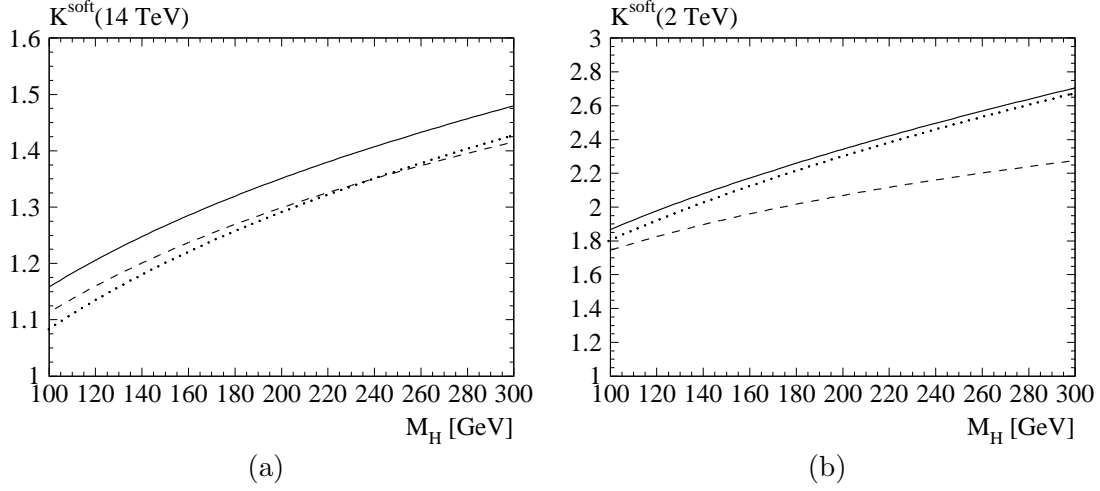


Figure 4: K factor as defined in Eq. (30), using the purely soft approximation of Eq. (25). Dashed and solid lines correspond to NLO and NNLO, respectively. The dotted line represents the approximate result $\bar{\sigma}_{gg}^{\text{soft}}$ of [10]. (a): $\sqrt{S} = 14 \text{ TeV}$, (b): $\sqrt{S} = 2 \text{ TeV}$, where \sqrt{S} is the CMS energy of the proton-proton system.

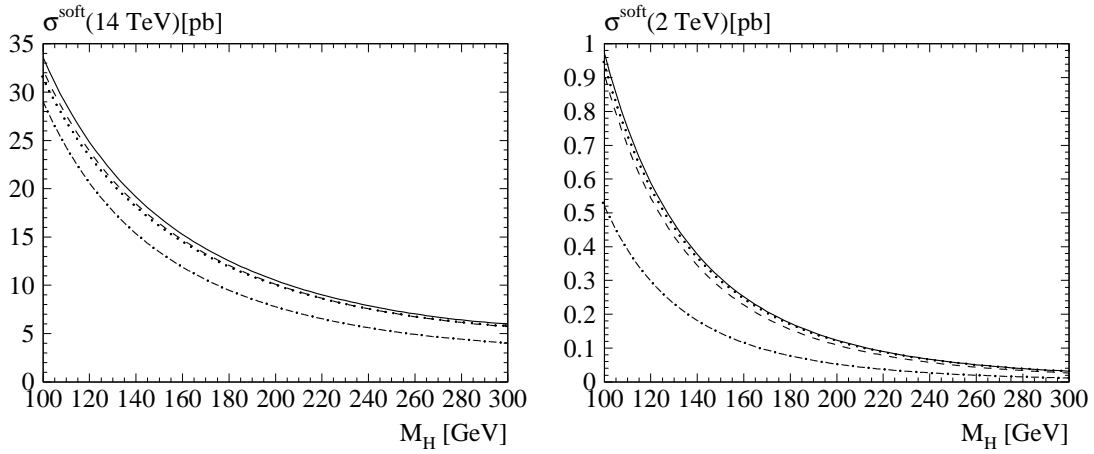


Figure 5: Cross section $\sigma(pp \rightarrow H + X)$ in the purely soft approximation (*cf.* caption of Fig. 4). Dash-dotted, dashed, and solid line correspond to LO, NLO, and NNLO results obtained from Eq. (25). The dotted line is the soft part of the NNLO approximation of ref. [10]. (a): $\sqrt{S} = 14 \text{ TeV}$, (b): $\sqrt{S} = 2 \text{ TeV}$.

correction. Thus, it will be necessary to compute the full NNLO correction, including the hard scattering terms, before one could conclude that the gluon fusion process is under control.

Until such time as the full calculation is available, we rely on the estimate of ref. [10] which points out that the hard scattering corrections at NLO are dominated by formally sub-leading terms of the form $\ln^i(1-x)$ and then estimates the NNLO correction including these sub-leading terms. We write their result as

$$\bar{\sigma}_{gg} = \bar{\sigma}_{gg}^{\text{soft}} + \bar{\sigma}_{gg}^{\text{sl}}. \quad (31)$$

$\bar{\sigma}_{gg}$ is generated from an expansion of a one-loop resummation formula and naturally the analytic form of $\bar{\sigma}_{gg}^{\text{soft}}$ differs from the actual NNLO result given in Eq. (25). Similarly, the (formally sub-leading, but numerically dominant) part $\bar{\sigma}_{gg}^{\text{sl}}$ is only an approximation of the actual, as yet unknown expression. In the case of Drell-Yan production, the result of ref. [10] *including* the corresponding sub-leading terms $\bar{\sigma}_{q\bar{q}}^{\text{sl}}$ reproduces the full answer [30] to within less than 5%. However, as can be seen in Fig. 4, the *soft* terms generated for Higgs productions are not particularly accurate representations of the true NNLO soft terms, especially at LHC energies.

With these caveats, we present an estimate of the full result by combining our result for the soft correction with the approximate, formally sub-leading logarithmic terms of ref. [10]. That is, we are going to add $\bar{\sigma}_{gg}^{\text{sl}}$ of Eq. (31) to our Eq. (25) and write:

$$\tilde{\sigma}_{gg}^{(i),\text{soft+sl}} = \hat{\sigma}_{gg}^{(i),\text{soft}} + \bar{\sigma}_{gg}^{(i),\text{sl}}, \quad i = 1, 2, \quad (32)$$

where [10]

$$\begin{aligned} \bar{\sigma}_{gg}^{(1),\text{sl}} &= -24 \ln(1-x), \\ \bar{\sigma}_{gg}^{(2),\text{sl}} &= -144 \ln^3(1-x) + \ln^2(1-x) (138 - 216 l_H - 4 n_f) \\ &\quad + \ln(1-x) (-132 + 138 l_H - 72 l_H^2 - 4 l_H n_f + 144 \zeta_2). \end{aligned} \quad (33)$$

Again, one must be very cautious about phenomenological interpretation of this result, because of the aforementioned approximate nature of $\bar{\sigma}_{gg}^{(2),\text{sl}}$.

In Fig. 6 we show the corresponding K -factors $K_{\text{NLO}}^{\text{soft+sl}}$ and $K_{\text{NNLO}}^{\text{soft+sl}}$ for a proton-proton CMS energy of (a) 14 TeV and (b) 2 TeV. By comparing to Fig. 4 one can see that the sub-leading terms clearly dominate the cross section. Fig. 7 shows the effect of the approximate sub-leading terms on the total cross section. One should bear in mind that the agreement of the solid and dotted lines in these two figures is due to the dominance of $\bar{\sigma}_{gg}^{(2),\text{sl}}$ which has been added both to our $\hat{\sigma}_{gg}^{(2),\text{soft}}$ and the approximate $\bar{\sigma}_{gg}^{(2),\text{soft}}$. If the approximation of ref. [10] is an accurate representation of reality, these figures indicate (at best) a very slow perturbative convergence of the total cross section.

5 Conclusions

The partonic cross section $gg \rightarrow H + X$ has been calculated to NNLO in the limit of soft emission. The resulting hadronic Higgs production rate exhibits well-behaved perturbative convergence properties. However, the effects of soft emission are expected to be

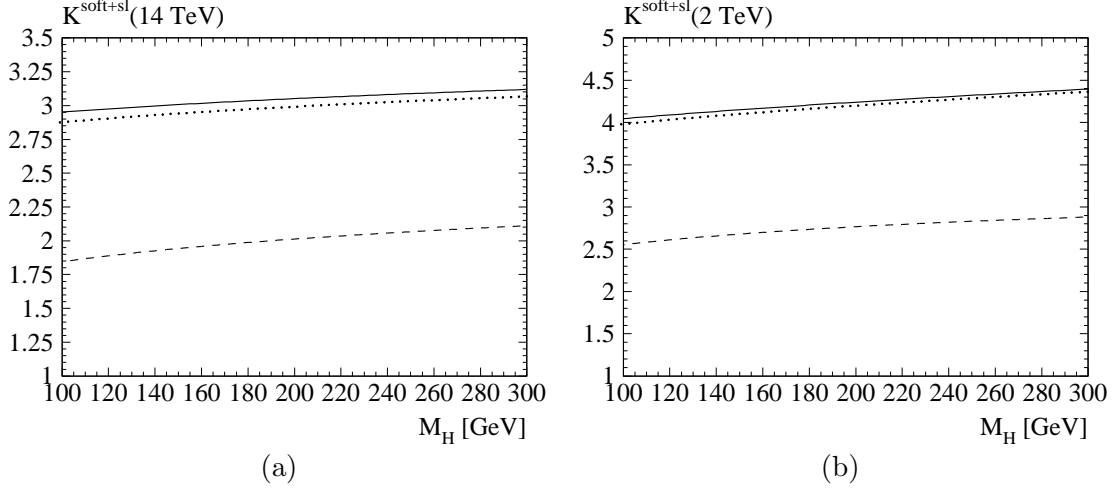


Figure 6: K factor as defined in Eq. (30), including soft and “sub-leading” terms, *i.e.* using Eq. (32) for the dashed and solid curves, and Eq. (31) (with $\bar{\sigma}_{gg}^{\text{soft}}$ extracted from [10]) for the dotted one.

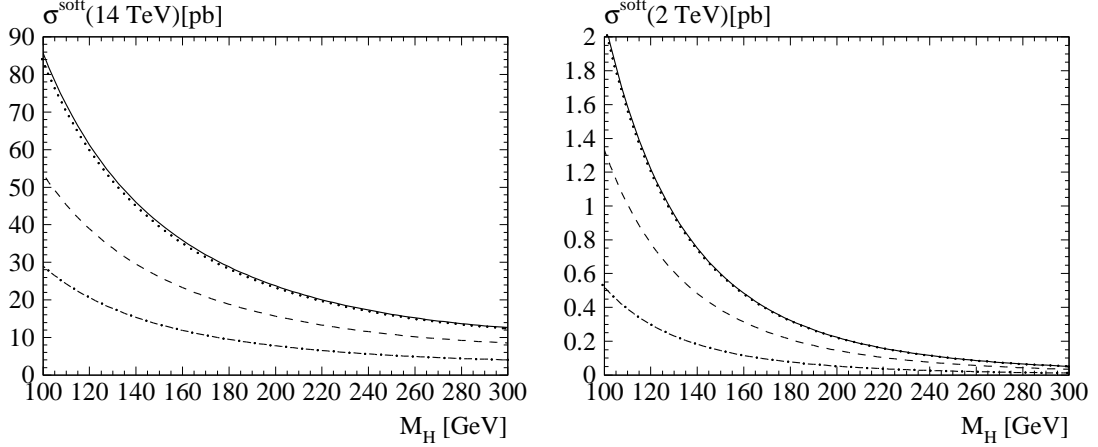


Figure 7: Cross section $\sigma(pp \rightarrow H + X)$ including soft and “sub-leading” terms (*cf.* caption of Fig. 6). Dash-dotted, dashed, and solid line correspond to LO, NLO, and NNLO results obtained from Eq. (25). The dotted line is the NNLO result based on the approximation given in [10]. (a): $\sqrt{S} = 14 \text{ TeV}$, (b): $\sqrt{S} = 2 \text{ TeV}$.

significantly smaller than the formally non-leading contributions $\propto \ln^i(1-x)$, for which an approximate result has been obtained in ref. [10]. This makes the complete evaluation of the NNLO corrections even more imperative.

Acknowledgments

We would like to thank S. Dawson and W. Vogelsang for many helpful discussions. The work of R.V.H. is supported by *Deutsche Forschungsgemeinschaft* and that of W.B.K. by the United States Department of Energy under grant DE-AC02-98CH10886.

References

- [1] P. Igo-Kemenes, talk given at LEPC meeting, 3 November, 2000;
The ALEPH Collaboration, *Phys. Lett. B* **495** (2000) 1;
The L3 Collaboration, *Phys. Lett. B* **495** (2000) 18;
The DELPHI Collaboration, *Phys. Lett. B* **499** (2001) 23;
The OPAL Collaboration, *Phys. Lett. B* **499** (2001) 38.
- [2] A. Straessner, talk given at XXXVth Rencontres de Moriond, March 2000;
D. Strom, talk given at RADCOR-2000, September 2000.
- [3] S. Heinemeyer, W. Hollik, G. Weiglein, *Eur. Phys. J. C* **9** (1999) 343.
- [4] M. Carena, *et al.*, Report of the Tevatron Higgs Working Group, hep-ph/0010338.
- [5] S. Dawson, *Nucl. Phys. B* **359** (1991) 283;
A. Djouadi, M. Spira, P.M. Zerwas, *Phys. Lett. B* **264** (1991) 440.
- [6] D. Graudenz, M. Spira, P.M. Zerwas, *Phys. Rev. Lett.* **70** (1993) 1372;
M. Spira, A. Djouadi, D. Graudenz, P.M. Zerwas, *Nucl. Phys. B* **453** (1995) 17.
- [7] F. Wilczek, *Phys. Rev. Lett.* **39** (1977) 1304;
J. Ellis, M.K. Gaillard, D.V. Nanopoulos, C.T. Sachrajda, *Phys. Lett. B* **83** (1979) 339;
H. Georgi, S. Glashow, M. Machacek, D.V. Nanopoulos, *Phys. Rev. Lett.* **40** (1978) 692;
T. Rizzo, *Phys. Rev. D* **22** (1980) 178.
- [8] A. Vainshtein, M. Voloshin, V. Zakharov, M. Shifman, *Sov. J. Nucl. Phys.* **30** (1979) 711;
A. Vainshtein, V. Zakharov, M. Shifman, *Sov. Phys. Usp.* **23** (1980) 429;
M. Voloshin, *Sov. J. Nucl. Phys.* **44** (1986) 478.
- [9] K.G. Chetyrkin, B.A. Kniehl, M. Steinhauser, *Nucl. Phys. B* **510** (1998) 61;
Phys. Rev. Lett. **79** (1997) 353.
- [10] M. Krämer, E. Laenen, M. Spira, *Nucl. Phys. B* **511** (1998) 523.
- [11] T. Matsuura, S.C. van der Marck, W.L. van Neerven, *Nucl. Phys. B* **319** (1989) 570.
- [12] V.P. Spiridonov, Rep. No. INR P-0378 (Moscow, 1984);
V.P. Spiridonov, K.G. Chetyrkin, *Yad. Fiz.* **47** (1988) 818.
- [13] R.V. Harlander, *Phys. Lett. B* **492** (2000) 74.
- [14] P.A. Baikov, V.A. Smirnov, *Phys. Lett. B* **477** (2000) 367.

- [15] F.V. Tkachov, *Phys. Lett.* **B 100** (1981) 65;
K.G. Chetyrkin, F.V. Tkachov, *Nucl. Phys.* **B 192** (1981) 159.
- [16] J.A.M. Vermaseren, Rep. No. NIKHEF-00-0032, math-ph/0010025.
- [17] S.A. Larin, F.V. Tkachov, J.A.M. Vermaseren, Rep. No. NIKHEF-H/91-18 (Amsterdam, 1991).
- [18] C.R. Schmidt, *Phys. Lett.* **B 413** (1997) 391;
C.R. Schmidt, private communication.
- [19] Z. Bern, D.A. Kosower, *Nucl. Phys.* **B 379** (1992) 451.
- [20] W.B. Kilgore, in preparation.
- [21] S. Dawson, R.P. Kauffman, *Phys. Rev. Lett.* **68** (1992) 2273;
R.P. Kauffman, S.V. Desai, D. Risal, *Phys. Rev.* **D 55** (1997) 4005, *Phys. Rev.* **D 58** (1998) 119901, Erratum.
- [22] G. Altarelli, G. Parisi, *Nucl. Phys.* **B 126** (1977) 298;
G. Curci, W. Furmanski, R. Petronzio, *Nucl. Phys.* **B 175** (1980) 27.
- [23] R.K. Ellis, W. Vogelsang, hep-ph/9602356.
- [24] S. Catani, *Phys. Lett.* **B 427** (1998) 161.
- [25] R.V. Harlander, W.B. Kilgore, Proc. of the DPF2000 meeting, Columbus, Ohio, 9-12 Aug 2000; hep-ph/0012176.
- [26] Z. Bern, V. Del Duca, W.B. Kilgore, C.R. Schmidt, *Phys. Rev.* **D 60** (1999) 116001.
- [27] G. Sterman, *Nucl. Phys.* **B 281** (1987) 310;
D. Appell, P. Mackenzie, G. Sterman, *Nucl. Phys.* **B 309** (1988) 259;
S. Catani, L. Trentadue, *Nucl. Phys.* **B 327** (1989) 323; *ibid.* **B353** (1991) 183;
S. Catani, G. Marchesini, B.R. Webber, *Nucl. Phys.* **B 349** (1991) 635.
- [28] A. Vogt, INLO-PUB 10/00, hep-ph/0010146.
- [29] H.L. Lai, *et al.* (CTEQ Collaboration), *Eur. Phys. J.* **C 12** (2000) 375.
- [30] R. Hamberg, T. Matsuura, W.L. van Neerven, *Nucl. Phys.* **B 359** (1991) 343;
E. Zijlstra, W.L. van Neerven, *Nucl. Phys.* **B 382** (1992) 11.